Mod Rheumatol
DOI 10.1007/s10165-009-0249-y

CASE REPORT

A case of familial Mediterranean fever associated with compound heterozygosity for the pyrin variant L110P-E148Q/M680I in Japan

Koichi Oshima · Kazuko Yamazaki · Yoichi Nakajima · Akari Kobayashi · Tomochika Kato · Osamu Ohara · Kazunaga Agematsu

Received: 18 August 2009 / Accepted: 23 October 2009

Abstract Familial Mediterranean fever (FMF) is an autosomal recessive disorder characterized by recurrent and self-limited fever attacks and serositis/arthritis. The M694V, M694I, M680I, V726A, and E148Q mutations in *MEFV*, the gene responsible for FMF, account for most FMF cases in Mediterranean populations. In Japan, M694I and E148Q are most frequently detected; M694V, M680I, and V726A have not been identified so far. We report the first case of FMF associated with M680I in Japan.

Keywords Familial Mediterranean fever · M680I · MEFV

Introduction

Familial Mediterranean fever (FMF) is an autosomal recessive disorder that is particularly common in Mediterranean populations [1]. It is characterized by recurrent and self-limited attacks of fever, serositis or arthritis and subsequent secondary amyloidosis [1–3]. The gene responsible for FMF-the Mediterranean fever gene (*MEFV*)-has been mapped to chromosome 16p13.3 [4–6]. It consists of 10 exons and encodes a protein comprising 781 amino acids called pyrin or marenostrin, which is expressed mainly in granulocytes and monocytes [4, 5]. So far, 184 mutations and polymorphisms of this gene have been identified [7]. Five common mutations (M694V, M694I, M680I, V726A, and E148Q) account for the vast majority of FMF mutations [8–10]. The clinical symptoms of FMF vary according to the mutations of *MEFV*. The M694V homozygote and compound heterozygote for M694V are associated with greater disease severity [11, 12]. Notably, E148Q is found in 16–25% of normal individuals in Japan [13], and it is known that compound heterozygous mutations of E148Q with M694V, M694I, M680I or V726A cause FMF.

In Japanese individuals, FMF is an extremely rare disease because of the low allele frequencies of the disease-causing mutations [13]. E148Q/M694I seem to be the most frequent alleles in Japanese FMF patients [13–15]. The M694V, M680I, and V726A mutations have not been found in Japan so far; herein, we report the first case in Japan of FMF in a patient who is compound heterozygote for L110P–E148Q/M680I.

Case report

A 7-year-old Japanese boy was brought to our hospital in 2007 for periodic fever accompanied by chest pain. He had experienced fever and chest pain once a year since the age of 3 years. The fever and chest pain continued for about 3 days after onset, and then disappeared spontaneously.

K. Oshima (✉) · O. Ohara
Laboratory for Immunogenomics, Research Center for Allergy and Immunology, RIKEN, Yokohama Institute, Yokohama, Japan
e-mail: oshima-k@umin.ac.jp

K. Yamazaki · K. Agematsu
Department of Infection and Host Defense, Shinshu University Graduate School of Medicine, Shinshu University School of Medicine, Matsumoto, Japan

Y. Nakajima · A. Kobayashi · T. Kato
Department of Pediatrics, Toyokawa City Hospital, Toyokawa, Japan

O. Ohara
Department of Human Genome Technology, Kazusa DNA Research Institute, Kisarazu, Japan

Published online: 08 December 2009

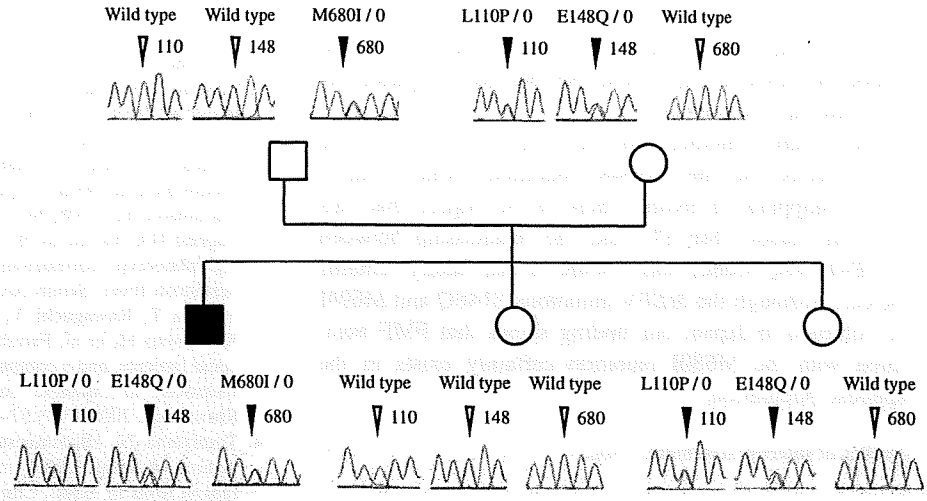

Fig. 1 Pedigree and chromatograms of the *MEFV* gene at amino acid positions 110, 148, and 680. *Black arrowheads* show heterozygous mutations for L110P, E148Q or M680I

None of his family members had these symptoms. From the age of 6 years, he experienced these symptoms about once every 2 months. At the time of the fever attack, he could not breathe deeply due to the chest pain. Subsequently rapid shallow breathing was recognized. Laboratory examinations showed mild leucocytosis (13,200 WBCs/μl) and elevated levels of C-reactive protein (CRP) (5.9 mg/dl) during an episode. Chest X-ray and electrocardiography revealed no abnormalities, and the patient did not have arthritis or rashes. Because he met the criteria for FMF based upon the Tel Hashomer criteria [2], we made a clinical diagnosis of FMF. After obtaining informed consent, we performed a genomic search for *MEFV*. Since the patient was found to be heterozygous for L110P–E148Q/M680I (Fig. 1), FMF was confirmed by the mutation in the hot spot of *MEFV*. The episodes were successfully prevented by administration of colchicine (0.25 mg/day).

Identification of M680I

After informed consent was obtained, the DNA of the patient, his parents, and 2 sisters was extracted from their peripheral blood mononuclear cells. The coding exons and flanking intronic sequences of the *MEFV* gene were amplified by polymerase chain reaction (PCR). The sequences of the PCR primers are available on request. The PCR products were treated using an ExoSAP-IT kit (GE Healthcare, Amersham, UK), and then analyzed by direct sequencing with an ABI 3130 DNA sequencer (Perkin-Elmer, Foster City, CA).

The results of the analysis are shown in Fig. 1. The L110P, E148Q, and M680I mutations were found in the patient. The patient's father was heterozygous only for the M680I mutation, and his mother carried the L110P and E148Q mutations. On the basis of the mutations carried by the parents, the patient was found to be heterozygous for L110P–E148Q/M680I. These mutations were not detected in his one sister, and his younger sister was heterozygous for L110P–E148Q. Interestingly, his mother and elder sister were heterozygous for the G304R mutation, which cause exon 2 skipping in pyrin (data not shown).

Discussion

Recently, a meta-analysis study on the founder populations (Jews, Armenians, Arabs, and Turks) for *MEFV* mutations revealed that the most frequent mutations detected in FMF patients are M694V (39.6%), V726A (13.9%), M680I (11.4%), E148Q (3.4%), and M694I (2.9%) [9]. The 4 major disease-causing mutations (M694V, M694I, M680I, and V726A) in exon 10 of *MEFV* have low allele frequencies in normal Japanese individuals [13]. Even for M694I, which seems to be the most common mutation in Japanese FMF patients [15], allele frequency was below 0.001 [13]. We recently reported that the common *MEFV* mutation patterns were E148Q/M694I (25.0%), L110P–E148Q/M694I (17.5%), and M694I alone (17.5%), and that the M694V, M680I or V726A mutations were not found in 80 Japanese FMF patients [15]. Some reports indicate that homozygous or compound heterozygous M680I mutations are associated with a moderate phenotype of the disease [16, 17]. Moreover, previous reports indicate that the M680I mutation, commonly seen in Armenians, is associated with a milder phenotype of the disease and lower frequency of amyloidosis [18, 19]. On the other hand, FMF patient heterozygous for the M680I gene mutation was reported to have developed nephritic syndrome [20]. Although we did not find abnormalities in chest imaging findings at the time of the fever attack, we strongly suspected presence of thoracic serositis because chest pain

accompanied by rapid shallow breathing are typical concomitant symptoms of FMF. Our patient is the first with the M680I mutation in Japan, and he showed comparatively mild clinical symptoms.

The patient's mother and one sister were found to be heterozygous for the G304R mutation, which causes exon 2 skipping in pyrin. There is no report that this mutation causes FMF [7], and the relationship between L110P–E148Q/M680I and G304R in this family remains unclear. Although the *MEFV* mutations E148Q and M694I are common in Japan, our finding shows that FMF associated with the M680I mutation certainly exists in the Japanese population.

Conflict of interest statement None.

References

1. Sohar E, Gafni J, Pras M, Heller H. Familial Mediterranean fever. A survey of 470 cases and review of the literature. Am J Med. 1967;43(2):227–53.
2. Livneh A, Langevitz P, Zemer D, Zaks N, Kees S, Lidar T, et al. Criteria for the diagnosis of familial Mediterranean fever. Arthritis Rheum. 1997;40(10):1879–85.
3. Ben-Chetrit E, Levy M. Familial Mediterranean fever. Lancet. 1998;351(9103):659–64.
4. Ancient missense mutations in a new member of the RoRet gene family are likely to cause familial Mediterranean fever. The International FMF Consortium. Cell. 1997;90(4):797–807.
5. French FMFC. A candidate gene for familial Mediterranean fever. Nat Genet. 1997;17(1):25–31.
6. Bernot A, da Silva C, Petit JL, Cruaud C, Caloustian C, Castet V, et al. Non-founder mutations in the MEFV gene establish this gene as the cause of familial Mediterranean fever (FMF). Hum Mol Genet. 1998;7(8):1317–25.
7. Infevers. The registry of Familial Mediterranean Fever (FMF) and hereditary auto-inflammatory disorders mutations. http://fmf.igh.cnrs.fr/ISSAID/infevers/ (2009).
8. Booth DR, Gillmore JD, Booth SE, Pepys MB, Hawkins PN. Pyrin/marenostrin mutations in familial Mediterranean fever. QJM. 1998;91(9):603–6.
9. Papadopoulos VP, Giaglis S, Mitroulis I, Ritis K. The population genetics of familial mediterranean fever: a meta-analysis study. Ann Hum Genet. 2008;72(Pt 6):752–61.
10. Touitou I. Standardized testing for mutations in familial Mediterranean fever. Clin Chem. 2003;49(11):1781–2.
11. Inal A, Yilmaz M, Kendirli SG, Altintas DU, Karakoc GB. The clinical and genetical features of 124 children with Familial Mediterranean fever: experience of a single tertiary center. Rheumatol Int. 2008;29(11):1279–85.
12. Majeed HA, El-Shanti H, Al-Khateeb MS, Rabaiha ZA. Genotype/phenotype correlations in Arab patients with familial Mediterranean fever. Semin Arthritis Rheum. 2002;31(6):371–6.
13. Sugiura T, Kawaguchi Y, Fujikawa S, Hirano Y, Igarashi T, Kawamoto M, et al. Familial Mediterranean fever in three Japanese patients, and a comparison of the frequency of MEFV gene mutations in Japanese and Mediterranean populations. Mod Rheumatol. 2008;18(1):57–9.
14. Tomiyama N, Higashiuesato Y, Oda T, Baba E, Harada M, Azuma M, et al. MEFV mutation analysis of familial Mediterranean fever in Japan. Clin Exp Rheumatol. 2008;26(1):13–7.
15. Tsuchiya-Suzuki A, Yazaki M, Nakamura A, Yamazaki K, Agematsu K, Matsuda M, et al. Clinical and Genetic Features of Familial Mediterranean Fever in Japan. J Rheumatol. 2009; 36(8):1671–6.
16. Gershoni-Baruch R, Brik R, Shinawi M, Livneh A. The differential contribution of MEFV mutant alleles to the clinical profile of familial Mediterranean fever. Eur J Hum Genet. 2002; 10(2):145–9.
17. Yalcinkaya F, Cakar N, Misirlioglu M, Tumer N, Akar N, Tekin M, et al. Genotype-phenotype correlation in a large group of Turkish patients with familial Mediterranean fever: evidence for mutation-independent amyloidosis. Rheumatology (Oxford). 2000;39(1):67–72.
18. Pras M. Familial Mediterranean fever: from the clinical syndrome to the cloning of the pyrin gene. Scand J Rheumatol. 1998;27(2):92–7.
19. Schwabe AD, Peters RS. Familial Mediterranean fever in Armenians. Analysis of 100 cases. Medicine (Baltimore). 1974;53(6):453–62.
20. Fisher PW, Ho LT, Goldschmidt R, Semerdjian RJ, Rutecki GW. Familial Mediterranean fever, inflammation and nephrotic syndrome: fibrillary glomerulopathy and the M680I missense mutation. BMC Nephrol. 2003;4:6.

Retrovirology

BioMed Central

Research

Open Access

DNA double strand break repair enzymes function at multiple steps in retroviral infection

Yasuteru Sakurai[1,2], Kenshi Komatsu[3], Kazunaga Agematsu[4] and Masao Matsuoka*[1]

Address: [1]Laboratory of Virus Control, Institute for Virus Research, Kyoto University, 53 Shogoin Kawahara-cho, Sakyo-ku, Kyoto 606-8507, Japan, [2]Laboratory of Cell Regulation and Molecular Network, Graduate School of Biostudies, Kyoto University, Kyoto 606-8501, Japan, [3]Department of Genome Repair Dynamics, Radiation Biology Center, Kyoto University, Yoshidakonoe-cho, Sakyo-ku, Kyoto 606-8501, Japan and [4]Department of Infection and Host Defense, Graduate School of Medicine, Shinshu University, 3-1-1, Asahi, Matsumoto, Nagano 390-8621, Japan

Email: Yasuteru Sakurai - ysakurai@virus.kyoto-u.ac.jp; Kenshi Komatsu - komatsu@house.rbc.kyoto-u.ac.jp; Kazunaga Agematsu - agemts_k@shinshu-u.ac.jp; Masao Matsuoka* - mmatsuok@virus.kyoto-u.ac.jp

* Corresponding author

Published: 15 December 2009

Retrovirology 2009, 6:114 doi:10.1186/1742-4690-6-114

Received: 9 September 2009
Accepted: 15 December 2009

This article is available from: http://www.retrovirology.com/content/6/1/114

Abstract

Background: DNA double strand break (DSB) repair enzymes are thought to be necessary for retroviral infection, especially for the post-integration repair and circularization of viral cDNA. However, the detailed roles of DSB repair enzymes in retroviral infection remain to be elucidated.

Results: A GFP reporter assay showed that the infectivity of an HIV-based vector decreased in ATM- and DNA-PKcs-deficient cells when compared with their complemented cells, while that of an MLV-based vector was diminished in Mre11- and DNA-PKcs-deficient cells. By using a method based on inverse- and Alu-PCR, we analyzed sequences around 3' HIV-1 integration sites in ATM-, Mre11- and NBS1- deficient cells. Increased abnormal junctions between the HIV-1 provirus and the host DNA were found in these mutant cell lines compared to the complemented cell lines and control MRC5SV cells. The abnormal junctions contained two types of insertions: 1) GT dinucleotides, which are normally removed by integrase during integration, and 2) inserted nucleotides of unknown origin. Artemis-deficient cells also showed such abnormalities. In Mre11-deficient cells, part of a primer binding site sequence was also detected. The 5' host-virus junctions in the mutant cells also contained these types of abnormal nucleotides. Moreover, the host-virus junctions of the MLV provirus showed similar abnormalities. These findings suggest that DSB repair enzymes play roles in the 3'-processing reaction and protection of the ends of viral DNA after reverse transcription. We also identified both 5' and 3' junctional sequences of the same provirus by inverse PCR and found that only the 3' junctions were abnormal with aberrant short repeats, indicating that the integration step was partially impaired in these cells. Furthermore, the conserved base preferences around HIV-1 integration sites were partially altered in ATM-deficient cells.

Conclusions: These results suggest that DSB repair enzymes are involved in multiple steps including integration and pre-integration steps during retroviral replication.

Background

Integration of viral DNA into the host genome is essential for retroviral replication. In this step, the integrase removes the two terminal nucleotides at each 3' end of the viral DNA (3'-processing) and catalyzes the joining of the processed end to the host DNA (strand transfer) [1]. Since the two ends attack the target DNA in a 5'-staggered fashion, single strand gaps between viral DNA and the target DNA are generated. Host DNA repair enzymes are thought to repair these gaps (post-integration repair). Additionally, unintegrated viral DNA is circularized to form two kinds of circular viral DNAs, 2-LTR circles and 1-LTR circles. Formation of these circular DNAs is also catalyzed by host DNA repair enzymes. Recent studies reported DNA double-strand break (DSB) repair enzymes as candidate catalysts for the post-integration repair and the circularization of viral DNA [2,3].

DSBs are the most serious damage that chromosomal DNA suffers, and must be repaired immediately and appropriately. When DSBs are generated in cellular DNA, ataxia-telangiectasia-mutated (ATM), a major molecular sensor of DSBs, directly binds to the damaged DNA and activates DSB repair pathways by phosphorylating target proteins [4,5]. One of the major targets is the MRN complex, which consists of Mre11, Rad50 and NBS1 [6]. This complex has recently been reported to further enhance ATM activation by recruiting ATM into the damaged site [7-9]. After detecting the damage, ATM activates two DSB repair pathways; homologous recombination (HR), and non-homologous end joining (NHEJ) [10]. In the NHEJ pathway, DNA-dependent protein kinase (DNA-PK), which consists of DNA-PK catalytic subunit (DNA-PKcs) and Ku, binds and holds the two ends of the break together. Then ligase IV/XRCC4/XLF carries out the ligation reaction [11,12]. When the ends are not suitable for direct ligation, Artemis nuclease often processes the ends [13].

Retroviral transduction into mutant cells lacking DNA-PK or ligase IV was reported to induce apoptosis [14-16], suggesting that NHEJ is involved in retroviral replication. Moreover, Lau *et al.* showed that an ATM-specific inhibitor suppressed integration of HIV-1 [17]. These reports support the involvement of DSB repair enzymes in post-integration repair. However, *in vitro* experiments showed only the involvement of the components of the single-strand break repair pathway [18,19]. In addition, some reports showed that DSB repair enzymes were only involved in the circularization of viral DNA [20,21]. However, the observation that Ku binds to retroviral preintegration complex (PIC) raises the possibility that DSB repair enzymes may play other roles in integration or pre-integration steps [20]. Thus, the detailed roles of these enzymes remain to be elucidated.

We report here that defects in DSB repair enzymes enhanced the formation of abnormal junctions between retroviral DNA and the host DNA. Moreover, we observed that the base preferences around HIV-1 integration sites partially changed in ATM-deficient cells. These results indicate that DSB repair enzymes are involved in multiple steps of retroviral replication.

Results

Effects of DSB repair enzymes on retroviral transduction efficiency

Previous reports demonstrated that retroviral infectivity decreased in cells lacking DSB repair enzymes such as ATM and DNA-PKcs [14,16,17]. To confirm whether the enzymes affect HIV-1 infectivity, mutant cell lines and complemented cell lines were transduced with an HIV-based vector encoding a GFP reporter gene. As shown in Figure 1A, the transduction efficiency was impaired in the mutant cells lacking ATM compared to the complemented cells, indicating that ATM is involved in HIV-1 transduc-

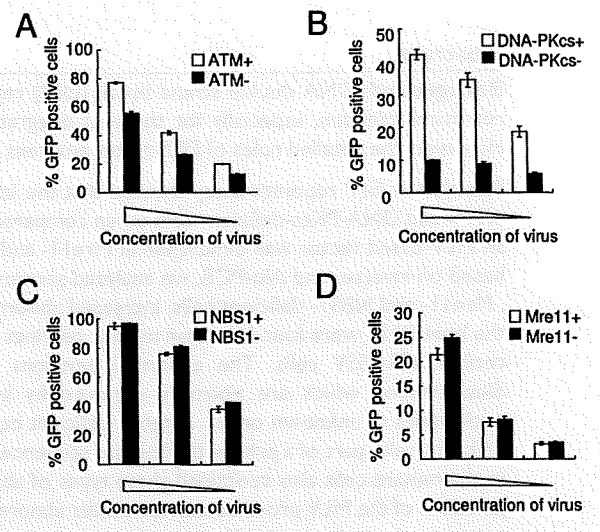

Figure 1

Transduction efficiency of the HIV-based vector into cells deficient in DSB repair enzymes. (A) ATM-deficient cells and ATM-complemented cells were transduced with three different dilutions of the HIV-based vector encoding a GFP reporter. Two days postinfection, the percentage of GFP-positive cells was determined by flow cytometry. (B-D) The influence of DNA-PKcs (B), NBS1 (C) and Mre11 (D) on transduction efficiency of the HIV-based vector was investigated by the same method as (A). Error bars represent +/- SD.

tion. We also found that DNA-PKcs-deficient M059J cells showed a significantly lower level of transduction efficiency compared to DNA-PKcs-positive M059K cells (Figure 1B), indicating that DNA-PKcs is also required for stable transduction of HIV-1.

The influences of NBS1 and Mre11 on retroviral infectivity were controversial in previous reports [21,22]. In our cell lines, NBS1 and Mre11 deficiencies did not influence transduction efficiency (Figure 1C and 1D), suggesting that the MRN complex might not affect HIV-1 transduction.

We also investigated whether defects in these DSB repair enzymes affected MLV infectivity by using an MLV-based vector encoding a GFP reporter gene. As for the HIV-based vector, the infectivity of the MLV-based vector significantly decreased in DNA-PKcs-deficient cells, indicating the conserved role of DNA-PKcs in retroviral infection (Additional file S1B). Mre11-deficient cells also showed impaired MLV infectivity compared to the complemented cells (Additional file S1D). However, infectivity of MLV vector remained intact in the mutant cells lacking NBS1, which is the other component of the MRN complex (Additional file S1C). This might be due to the different extents of deficiencies of Mre11 and NBS1. In contrast to the HIV-based vector, ATM-deficient cells showed similar transduction efficiency of the MLV-based vector compared to the complemented cells (Additional file S1A). These results suggest that DSB repair enzymes are differentially required for the stable transduction of HIV-1 and MLV.

Abnormal junctions between HIV-1 provirus and the host DNA in ATM-, Mre11-, NBS1- and Artemis-deficient cells

Since one of the potential targets of DNA repair enzymes is the junction between provirus and the host DNA [18,19,23], we postulated that abnormal junctions would be generated in cells deficient in DNA repair enzymes. We therefore analyzed the sequences of the host-virus junctions. After amplification of integration sites by *Alu* PCR, we used inverse PCR to amplify the sequences around the integration sites with primers specific to LTRs and *Alu* repeat elements [24]. With this method, we could identify integration sites efficiently, with few non-specific amplification products.

We analyzed 216 3' junctions between HIV-1 provirus and the host DNA in a control cell line, MRC5SV, and found one abnormal junction with a single nucleotide insertion, and seven junctions with deletions in viral DNA ends (Figure 2). In mutant cells lacking DSB repair enzymes, there were more abnormal junctions with inserted nucleotides between provirus and the host DNA. There were two different groups of abnormal nucleotides. One was a GT dinucleotides (or a G mononucleotide) adjacent to the provirus that is normally removed by integrase in 3'-processing. They did not originate from the host DNA. The other type of abnormal junction contained inserted nucleotides of unknown origin. The number of abnormal junctions with insertions was 1 of 216 (0.5%) events in the control cells, but 8 of 161 (5.0%) events in ATM-deficient cells (Figure 2 and Table 1). In ATM-complemented cells, 1 of 151 (0.7%) junctions had abnormal insertions, which was a significantly lower frequency than that of ATM-deficient cells. Although GFP reporter assays showed that defect of the MRN complex did not affect HIV-1 infectivity, the junctions in the MRN complex deficient cells also had abnormal insertions: 11 of 147 (7.5%) junctions in Mre11-deficient cells and 6 of 145 (4.1%) junctions in NBS1-deficient cells. It is of note that some of the abnormal junctions in Mre11-deficient cells also included 2, 4, 11, or 15 nucleotides of the primer binding site (PBS) sequences (Figure 2). In contrast, abnormal junctions with insertions were less frequent in Mre11-complemented cells (2 of 144: 1.4%) and NBS1- complemented cells (1 of 168: 0.6%). These results indicate that both Mre11 and NBS1 are indeed associated with HIV-1 replication. In contrast, in DNA-PKcs-deficient cells, only 3 of 153 (2.0%) junctions had abnormal insertions (Additional file S2), which is not a statistically significant difference compared to control MRC5SV cells.

Abnormal junctions with insertions were also found in 10 of 136 (7.4%) junctions in cells deficient in Artemis (Fig-

Table 1: The number of 3' abnormal junctions of the HIV-1 provirus

	ATM(-)	ATM(+)	Mre11(-)	Mre11(+)	NBS1(-)	NBS1(+)	Artemis(-)	MRC5SV
Insertions	8	1	11	2	5	1	9	1
Insertions + Deletions	0	0	0	0	1	0	1	0
Deletions	2	3	2	3	2	5	1	7
Total junctions	161	151	147	144	145	168	136	216
P value	0.012 (0.0046)	(0.80)	0.023 (0.00005)	(0.34)	0.035 (0.013)	(0.86)	(0.0003)	

The *P* values under the columns of the deficient cell lines are for comparison of the number of junctions with only insertions or both insertions and deletions to that of the corresponding complemented cell lines. The numbers in parentheses under the table represent the *P* values compared to the control MRC5SV cells.

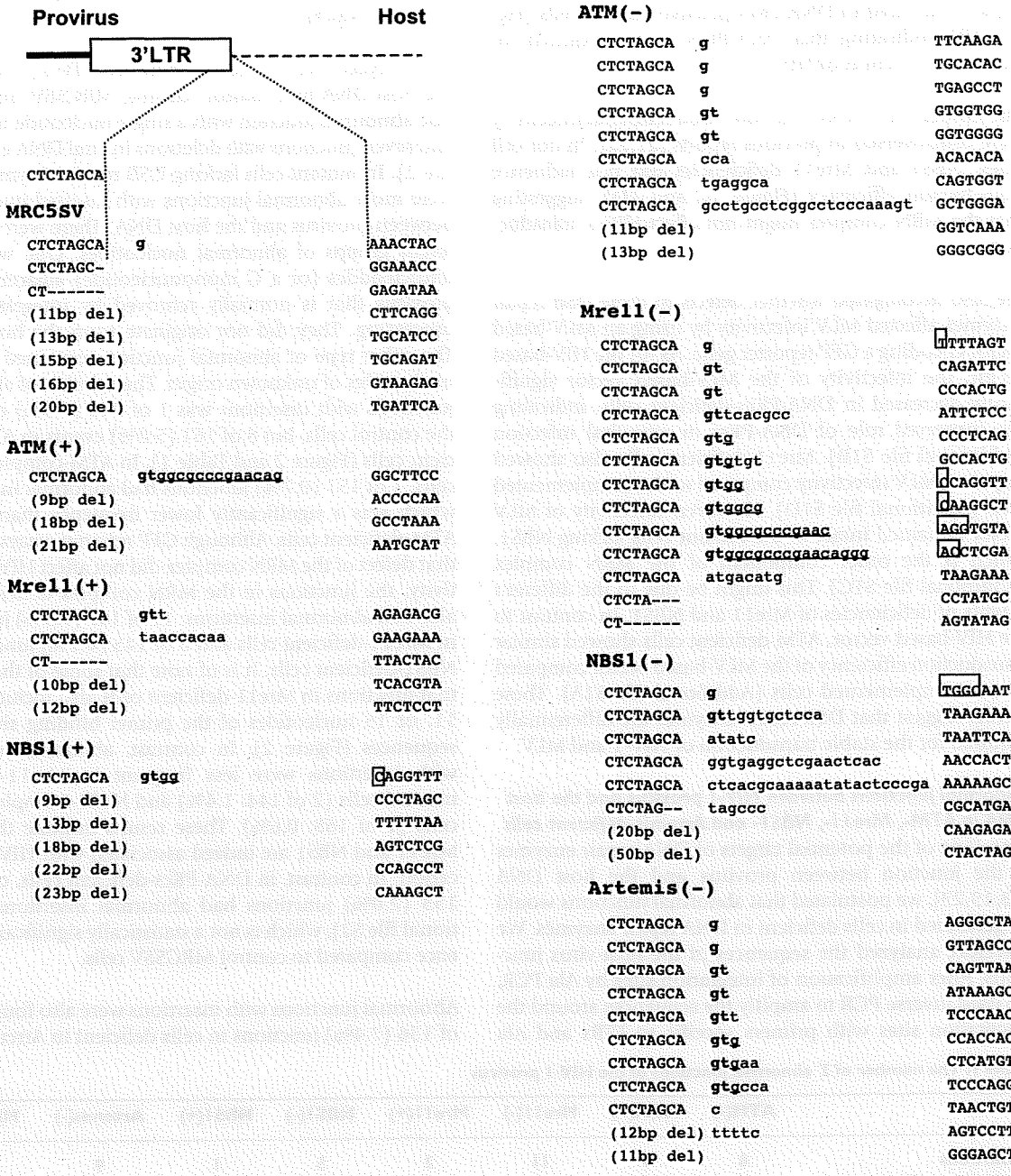

Figure 2

Abnormal 3' junctions of the HIV-1 provirus in DSB repair enzyme deficient cells. Junctions between the 3' end of the provirus and the host DNA were analyzed in control cells, mutant cell lines, and complemented cell lines transduced with the HIV-based vector. Inserted abnormal sequences are lowercased. Abnormal nucleotides corresponding to the GT dinucleotides processed by integrase are presented in bold. Partial primer binding site (PBS) sequences are underlined. Squares indicate the location of micro-homologies to the GT dinucleotides and/or PBS.

ure 2 and Table 1), which is a target of phosphorylation by ATM and DNA-PKcs [25,26]. Since Artemis-complemented cells could not be established, we could not conclude that these abnormalities observed in Artemis deficient cells were due to the deficiency of Artemis. However, the frequency was much higher than that of control MRC5SV cells (P = 0.0003), indicating the potential effects of Artemis on HIV-1 replication.

Some of the abnormal junctions also exhibited microhomologies in the host sequences, in which 1-4 nucleotides were identical to a part of the GT dinucleotides and/or the PBS sequence following the inserted part (Figure 2). This observation suggests that at least some proviruses with such abnormal junctions might be integrated by a recombination mechanism using these microhomologies.

5' junctional sequences in DSB repair enzymes-deficient cells

To investigate whether the abnormalities were common to both ends of provirus, we also analyzed the sequences of 5' junctions. The junctions between the HIV-1 5' LTR and the host DNA also exhibited similar abnormalities (Figure 3A). Abnormal nucleotides were observed in 10 of 164 (6.1%) junctions in ATM-deficient cells and 13 of 134 (9.7%) junctions in Mre11-deficient cells, compared to 2 of 178 (1.1%) junctions in MRC5SV cells (Figure 3B). In 5' junctions, the remaining nucleotides were AC dinucleotides, which are complementary to the GT dinucleotides detected in 3' junctions. In Mre11 deficient cells, 3' polypurine tract (PPT) sequences were also identified. Thus, defects in DSB repair enzymes enhanced the abnormal joining of both ends of the HIV-1 DNA.

Abnormal junctions of MLV provirus in DSB repair enzyme deficient cells

To determine whether these abnormalities are specific to HIV-1, we also analyzed sequences of the 3' junctions of the MLV provirus. Junctions with abnormal nucleotides increased from 5 of 228 (2.2%) events in Mre11-complemented cells to 20 of 256 (7.8%) events in Mre11-deficient cells (Figure 4). The abnormal junctions also included TT dinucleotides, which are usually removed by MLV integrase in 3'-processing. Taken together, these results show that defects in DSB repair enzymes increase abnormal host-virus junctions in both HIV-1 and MLV.

Junctional sequences at the both ends of provirus

To study whether both 5'- and 3'-junctions of the same provirus were abnormal, we analyzed both 5' and 3' junctional sequences of the same provirus. Since the method used in Figure 2, 3 and 4 could detect only one end of provirus, we next adopted a traditional inverse PCR method. We identified three HIV-1 proviruses with abnormal junc-

A

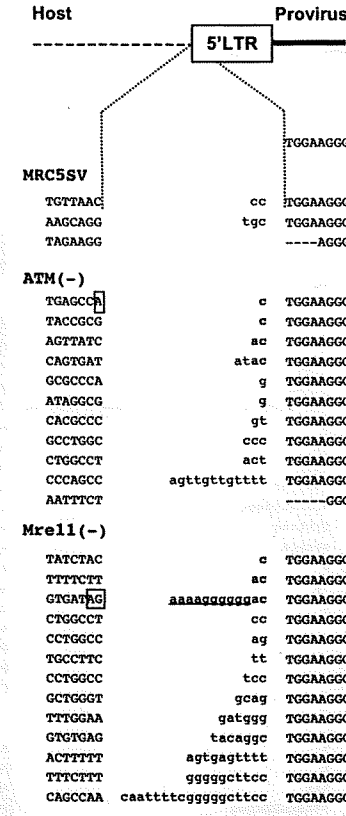

B

	MRC5Sv	ATM(-)	Mre11(-)
Insertions	**2**	**10**	**13**
Deletions	1	1	0
Total junctions	178	164	134
P value		0.013	0.0005

Figure 3
Abnormal 5' junctions of the HIV-1 provirus in DSB repair enzyme deficient cells. (A) Junctions between the 5' end of the provirus and the host DNA were analyzed in control and mutant cell lines transduced with the HIV-based vector. Inserted abnormal sequences are in lower case. Abnormal nucleotides corresponding to the sequence (AC) complementary to the GT dinucleotides processed by integrase are presented in bold. Partial polypurine tract (PPT) sequences are underlined, Squares indicate the location of micro-homologies to the AC dinucleotides and/or PPT. (B) The number of junctions with insertions or deletions. The *P* values under the table are for comparison of the number of junctions with insertions in each cell line to that of the control MRC5SV cells.

A

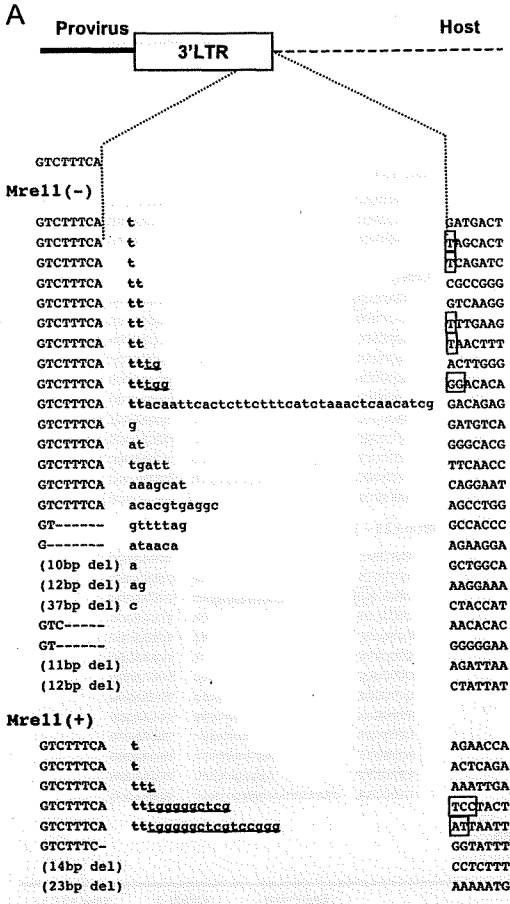

B

	Mre11(-)	Mre11(+)
Insertions	**15**	**5**
Insertions + Deletions	**5**	**0**
Deletions	4	3
Total junctions	256	228
P value	0.0053	

Figure 4
Abnormal 3' junctions of the MLV provirus in Mre11-deficient cells. (A) Junctions were analyzed in Mre11-deficient cells and Mre11-complemented cells transduced with the MLV-based vector. Abnormal nucleotides corresponding to dinucleotides (TT) processed by integrase are in bold. Underlined sequences indicate partial PBSs. Squares indicate the location of micro-homologies to TT dinucleotides and/or the PBS. (B) The number of junctions with insertions or deletions. The *P* values under the table are for comparison of the number of junctions with insertions in Mre11-deficient cells to that of Mre11-complemented cells.

tions in Mre11-deficient cells (Figure 5). All three proviruses had the abnormal nucleotides at the 3' junctions. A single G was inserted in case 1, while both GT dinucleotides and part of a PBS were inserted in cases 2 and 3. These 3' junctions also showed micro-homologies in the host sequences, confirming the abnormalities shown in Figure 2. However, the 5' junctions were intact in these proviruses, indicating that these 5' junctions were processed by integrase as per normal. We also found that the host sequence adjacent to the provirus contained short repeats in case 1 and 2. Although all of the other proviruses had 5-bp short repeats as reported previously (data not shown), case 1 and 2 contained 3-bp and 2-bp short repeats, respectively. Case 3 lacked short repeats. These results suggest that the integration of these proviruses was catalyzed by integrase, but in abnormal ways.

Altered base preference surrounding HIV-1 integration sites in cells lacking ATM

Retrovirus-specific base preferences in the immediate vicinity of integration sites have been reported [27-29]. Our findings of abnormal host-virus junctions prompted us to investigate whether deficiencies in DSB repair enzymes also influence these preference patterns. We analyzed the nucleotide frequencies for the 8 nucleotides downstream and the 4 nucleotides upstream of the 3' ends of HIV-1 proviruses without insertions and/or deletions (Figure 6B). As shown in Figures 6 and 7, we calculated P values at each position by χ^2 analysis comparing the base compositions in each cell line and the average base compositions in the human genome (A:29%, T:29%, G:21%, C:21%). At the positions with $P < 0.01$, the bases with high frequencies or low frequencies were focused and colored in Figure 6 and 7. Compared to the control MRC5SV cells and ATM-complemented cells, which showed a preference pattern similar to that in the previous report [28], ATM-deficient cells showed a partially altered pattern. In the position -2, the different patterns were found in ATM-deficient cells compared to control MRC5SV cells ($P < 0.0001$) or ATM-complemented cells ($P < 10^{-14}$). Especially, ATM-deficient cells showed higher frequency of G compared to the control MRC5SV cells and the complemented cells at the position -2. Similarly, integration sites for the 5' end of the provirus in ATM-deficient cells showed a changed preference pattern in position 7 compared to the control MRC5SV cells ($P < 0.001$), in which ATM-deficient cells showed a higher frequency of G (Figure 7B). Since the 5 bp sequence (positions 1 to 5) is duplicated next to the 3' and 5' ends of the provirus as short repeats, position 7 for the 5' end of the provirus corresponds to position -2 for the 3' end of the provirus. This indicates that the analyses at both ends of the provirus showed the same change, suggesting the influence of deficiency in ATM in the position. In contrast, NBS1- and Mre11-deficient cells showed no clear change

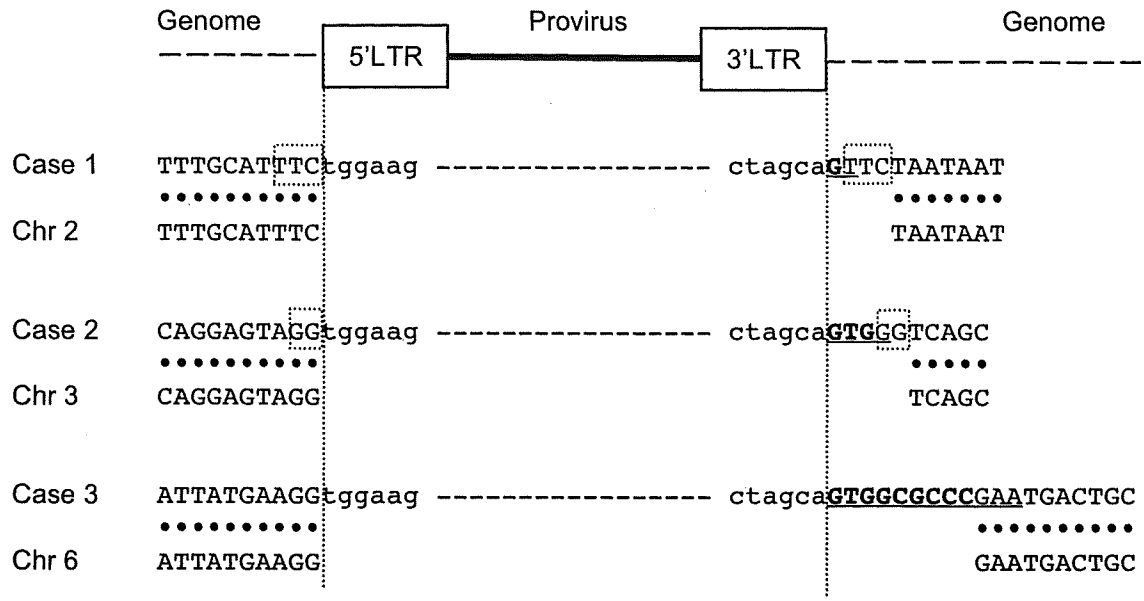

Figure 5
The 5' and 3' junctional sequences of the same HIV provirus in Mre11-deficient cells. Junctions between both ends of HIV provirus and the host DNA were analyzed together in Mre11-deficient cells transduced with the HIV-based vector. Three cases including abnormal junctions are shown. In each case, the integrated HIV provirus (top) and the host genome (bottom) are compared. Proviral sequences are in lower case. Inserted abnormal nucleotides are shown in bold. The GT dinucleotides and primer binding site (PBS) sequences are underlined. Squares indicate short repeats flanking the provirus.

in base preference (data not shown). Thus, deficiency in ATM partially influences the local base preference pattern surrounding HIV-1 integration sites.

Effects of the MRN complex on circularization of HIV-1 cDNA

Previous reports suggested that some DSB repair enzymes were involved in the formation of 2-LTR circles and 1-LTR circles [20,21]. To investigate whether the formation of abnormal host-virus junctions links to circularization of viral cDNA, we quantified total viral cDNA, 2-LTR circles and 1-LTR circles in Mre11-deficient cells and the complemented cells. Quantitative analyses of these viral cDNAs showed that the amount of all three types of viral cDNA was similar in the deficient cells and the complemented cells (Figure 8). This suggested that deficiency in the MRN complex did not influence the formation of viral circular DNAs at least in these cell lines.

Discussion

This study revealed that deficiencies in some DSB repair enzymes caused abnormalities surrounding retroviral integration sites. Although the GFP reporter assay indicated involvement of ATM and DNA-PKcs in HIV-1 infection consistent with previous reports [14,16,17], the sequence analyses of the host-virus junctions revealed that Mre11 and NBS1 were also involved in HIV-1 infection. In addition, both the GFP reporter assay and the sequence analysis showed the involvement of Mre11 in MLV infection. These results suggest that DSB repair enzymes are more important in retroviral infection than previously thought.

We found two kinds of abnormal junctions in ATM-, Mre11-, NBS1- and Artemis-deficient cells. One contained remnant dinucleotides, which are normally removed from the ends of viral DNA. These were identical to nucleotides processed in 3'-processing [30], which suggest that integrase could not completely process the terminal dinucleotides, or that the processed 3'-ends were repaired during integration. This abnormality suggests that ATM, the MRN complex and Artemis play roles in the 3'-processing activity of integrase and possibly the protection of the ends of viral DNA before strand transfer. In addition, abnormal junctions containing sequences derived from the PBS were found only in Mre11-deficient cells. As the tRNA primer is thought to be removed by the RNase H domain of reverse transcriptase (RT) [31,32], Mre11 may

A

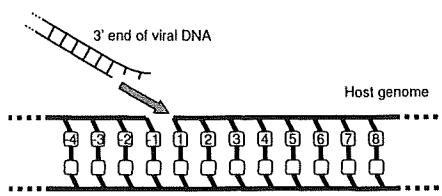

B

MRC5SV (207 sites)

	-4	-3	-2	-1	1	2	3	4	5	6	7	8
A	80	60	133	110	98	117	140	173	30	98	120	195
T	103	165	93	78	33	138	107	78	88	68	105	58
G	120	115	120	174	219	67	74	81	145	85	55	62
C	108	55	48	46	81	62	67	53	173	143	115	69
$-\log_{10}(P)$	0.6	9.0	3.8	8.1	18.5	4.1	3.3	9.3	12.6	2.7	2.2	15.4

ATM(+) (147 sites)

	-4	-3	-2	-1	1	2	3	4	5	6	7	8
A	84	59	108	99	75	82	120	148	33	94	138	176
T	106	178	115	61	40	185	110	101	91	94	75	54
G	97	87	139	194	188	58	91	65	130	68	45	65
C	117	62	29	62	130	49	68	68	175	149	136	94
$-\log_{10}(P)$	0.2	7.6	4.1	7.7	8.9	9.2	0.9	3.1	7.9	1.9	4.2	7.5

ATM(-) (151 sites)

	-4	-3	-2	-1	1	2	3	4	5	6	7	8
A	62	87	121	102	100	80	123	160	41	78	116	160
T	114	160	66	59	21	153	100	105	75	69	107	75
G	101	101	151	151	183	98	88	57	110	95	54	91
C	132	35	66	101	126	57	79	54	205	160	114	60
$-\log_{10}(P)$	1.7	5.9	3.5	2.9	10.4	3.8	0.6	5.6	10.8	5.2	1.5	4.5

Figure 6
The local base preferences surrounding 3' ends of HIV-1 proviruses integrated in ATM-deficient cells. (A) A schematic figure of the strand transfer reaction of HIV-1. The 3' end of viral DNA attacks the phosphodiester bond between positions -1 and 1 of the host DNA, and covalently joins to the position 1 nucleotide. (B) Base compositions around the integration sites in the control MRC5SV cells, ATM-complemented cells and ATM-deficient cells. The sequences represent the target DNA sequence before the viral DNA is inserted between the position 1 and -1. The 5 bp sequences (positions 1 to 5), which are duplicated next to both ends of the provirus, are boxed by blue lines. Each tabulated number represents the observed base frequency divided by the expected base frequency at each position. The expected base frequencies are average frequencies observed in human genome (A:29%, T:29%, G:21%, C:21%). The P values are obtained by χ^2 analysis comparing observed and expected base compositions at each position. At the positions with $P < 0.01$, frequencies < 60% and frequencies > 140% of expected frequencies are colored yellow and green, respectively.

regulate RT to cleave the tRNA correctly. It is noteworthy that a part of 3' PPT sequence of HIV-1, which is a primer sequence for the synthesis of the plus strand, was found at 5' junctions in Mre11 deficient cells. Inserted aberrant nucleotides of unknown origin were another junctional abnormality. Considering that one strand of viral DNA has already bound to the host DNA in the integration intermediate, it is likely that the inserted nucleotides were added at the viral DNA ends before strand transfer. It has been demonstrated that ATM and the MRN complex protect human telomeres, by capping them [33,34]. In addition, a report regarding telomere instability in Artemis-deficient cells suggests that Artemis also protects telomeres [35]. Given that telomeres and unintegrated retroviral DNA ends are similar, DSB repair enzymes including ATM, the MRN complex and Artemis may protect the ends of unintegrated viral DNA from aberrant nucleotide addition.

One reason for the inconsistency between the GFP reporter assay and the sequence analyses, particularly in Mre11 and NBS1, may be that the frequencies of the abnormalities at the host-virus junctions were low. Therefore, it was not detected by the GFP reporter assay. In addition, the GFP reporter assay could detect integrated provirus with abnormal junctions. Therefore, the GFP assay could not discriminate provirus with abnormal junctions from normally integrated provirus. It is possible that the integration efficiency of viral DNA with abnormal ends might be low compared with normal viral DNA, which might underestimate the frequencies of provirus with aberrant ends. Since the deficiencies of Mre11 and NBS1 in the mutant cell lines were reported to be only hypomorphic, the effects of their deficiencies are likely limited in this study [36]. However, the finding that the insertional abnormalities were more frequent in the deficient cell lines compared to the control cell lines indicates the existence of an association between retroviral infection and DSB repair enzymes including Mre11 and NBS1. This was also supported by one of the recent reports that identified host factors by genome-wide screening using an RNAi library [37]. In this report, the knockdown of Mre11 decreased retroviral infectivity.

The identification of the abnormal junctions prompted us to investigate how proviruses with such junctions were integrated. The micro-homologies in the host sequences suggest that integrase-independent recombination is involved in this step (Figure 2, 3 and 4). However, when both 5' and 3' junctional sequences of the same provirus were analyzed, only the 3' junctions of the provirus were abnormal while the 5' junctions were intact (Figure 5), suggesting the involvement of integrase in the establishment of these proviruses. In addition, although normal

A

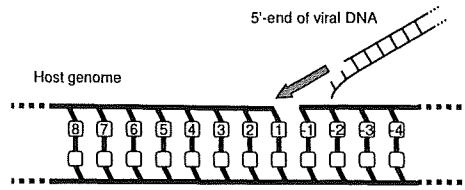

B

MRC5SV (175 sites)

	8	7	6	5	4	3	2	1	-1	-2	-3	-4
A	49	89	104	75	89	120	144	18	67	95	148	104
T	166	118	87	35	166	112	99	108	114	112	73	87
G	125	122	147	199	57	84	90	112	65	63	63	98
C	54	68	65	125	68	71	52	190	161	128	109	114
$-\log_{10}(P)$	9.0	1.3	2.4	12.7	6.5	1.1	3.5	13.4	4.7	1.5	3.9	0.2

ATM(-) (152 sites)

	8	7	6	5	4	3	2	1	-1	-2	-3	-4
A	77	104	113	75	84	100	132	25	64	100	159	104
T	157	93	91	27	170	116	91	100	98	109	82	102
G	78	150	119	216	60	72	88	119	88	50	47	110
C	75	53	75	119	66	107	81	185	166	138	97	81
$-\log_{10}(P)$	3.7	2.8	0.6	14.4	6.2	0.5	1.0	9.9	3.8	2.3	5.0	0.2

Figure 7
The local base preferences surrounding 5' ends of HIV-1 proviruses integrated in ATM-deficient cells. (A) A schematic figure of the strand transfer reaction of HIV-1. The 5' end of viral DNA attacks the phosphodiester bond between positions -1 and 1 of the host DNA, and covalently joins to the position 1 nucleotide. (B) Base compositions around the integration sites in the control MRC5SV cells and ATM-deficient cells. The sequences represent the target DNA sequence before the viral DNA is inserted between the position 1 and -1. The 5 bp sequences (positions 1 to 5), which are duplicated next to both ends of the provirus, are boxed by blue lines. Each tabulated number represents the observed base frequency divided by the expected base frequency at each position. The expected base frequencies are average frequencies observed in the human genome (A:29%, G:21%, C:21%). The P values are obtained by χ^2 analysis comparing observed and expected base compositions at each position. At the positions with $P < 0.01$, frequencies < 60% and frequencies > 140% of expected frequencies are colored yellow and green, respectively.

HIV-1 integration generates 5-bp short repeats flanking the provirus, the abnormal proviruses lacked short repeat or had aberrant (2- or 3-bp) short repeats. These findings suggest that these proviruses were established by impaired activity of integrase.

A

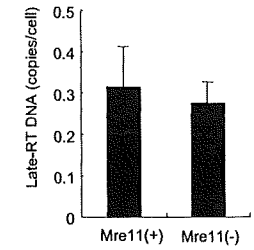

B

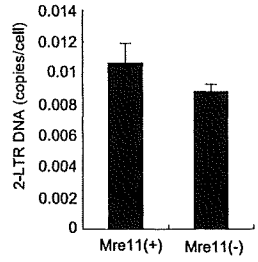

C

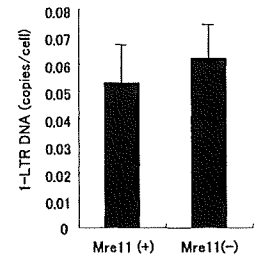

Figure 8
Quantification of viral cDNA in Mre11-deficient cells and the complemented cells. Mre11-deficient and complemented cells were transduced with the HIV-based vector, and the total DNA was extracted. By fluorescent-monitored quantitative PCR, total viral DNA (A), 2-LTR circles (B) and 1-LTR circles (C) were quantified. Error bars represent +/- SD.

There are inconsistencies in previous reports regarding the roles of DNA repair enzymes in retroviral replication [38-42]. This is partly because almost all of these studies were based on measuring the retroviral infectivity or apoptosis by retroviral transduction as was done in Figure 1 and S1. Such assays largely depend on the extent of deficiencies or the expression levels of the complemented proteins. The situation is further complicated by the fact that complete deletion of some DSB repair enzymes such as Mre11 and NBS1 is lethal, and there are only hypomorphic mutant cell lines [36]. In some reports, suppressed expression of LEDGF/p75, which is a critical host factor of HIV-1 replication, had no or only modest effect on HIV-1 infectivity [43,44]. However, biochemical assays and sequence analyses in the same cell lines in other studies revealed a strong association of LEDGF/p75 with HIV-1 replication, suggesting that the quantitative assays could not detect all abnormalities [45-47]. Indeed, our sequence analyses revealed abnormalities undetected by the GFP reporter assay in Mre11- and NBS1- deficient cells. These results

show the importance of qualitative assays to evaluate the involvement of host factors including DSB repair enzymes in retroviral replication.

Our sequence analyses also showed that deficiencies of DSB repair enzymes influenced HIV-1 integration site selection (Figure 6 and 7). In a recent and substantial effort to understand the mechanism of retroviral integration site selection, Holman *et al.* demonstrated virus-specific base preferences around retroviral integration sites by analyzing massive numbers of integration sites [28]. Our data showing partially altered patterns in ATM-deficient cells reveal that the preference pattern of HIV-1 is marginally influenced by ATM. Interestingly, a lack of ATM caused the appearance of a new base preference. As the new preference may limit the selection of a target DNA sequence, the appearance of the new preference is consistent with decreased HIV-1 infectivity in ATM-deficient cells.

Besides post-integration repair and circularization of viral cDNA, we propose additional possible roles for DSB repair enzymes. Given that Ku was reported to bind to retroviral PICs [20,22], DSB repair enzymes investigated in this study may also bind to PICs and directly regulate their activities. Although further studies are necessary to validate our models regarding the roles of DSB repair enzymes, this study suggests that DSB repair enzymes are involved in retroviral replication in more ways than previously thought. This study sheds light on novel links between DSB repair enzymes and retrovirus, and raises new questions about the detailed mechanism by which DSB repair enzymes control retroviral replication.

Conclusions

This study showed aberrant sequences surrounding retroviral integration sites in DSB repair enzyme deficient cells; increased abnormal nucleotides at the host-virus junctions and partially altered base preferences surrounding integration sites. These results suggest that DSB repair enzymes are involved in both retroviral integration and pre-integration steps.

Methods

Cell lines

293T cells and MRC5SV cells, an SV40-transformed human fibroblast line, were cultured in Dulbecco's modified Eagle's medium (DMEM) and were supplemented with 10% fetal bovine serum, 2 mM L-glutamine, 100 U/ml penicillin, and 50 μg/ml streptomycin. Adenovirus-transformed Artemis-deficient cells originated from RS-SCID patients and were cultured in DMEM [48]. ATM-deficient and ATM-complemented cells were established by transfecting empty vector and ATM expression vector, respectively, into an A-T cell line, AT5BIVA, as described previously [49], and cultured in DMEM containing 200 μg/ml hygromycin B (Calbiochem, San Diego, CA). NBS1-deficient and NBS1-complemented cells were established by transfecting empty vector and NBS1 expression vector, respectively, into an NBS cell line, GM7166VA7, as described previously [50], and cultured in DMEM containing 500 μg/ml G418 (Nacalai tesque, Kyoto, Japan). Mre11-deficient cells were established by transforming an ATLD2 cell line, D6809 (a generous gift from Dr. P. Concannon), by SV40, and the cells were cultured in DMEM. To obtain Mre11-complemented cells, Mre11-deficient cells were transfected with the Mre11 expression vector pCMV-Tag-Mre11, which was created by cloning Mre11 cDNA between the EcoRI and ApaI sites of pCMV-Tag 2B (Clontech, Mountain View, CA), and the cells were cultured in DMEM containing 500 μg/ml G418. For all experiments, we used antibiotic-free medium before 24 h of experiments.

Production of viral vectors

An HIV-based vector encoding a green fluorescent protein (GFP) reporter was produced as follows. 293T cells were transfected by TransFectin (Bio-Rad, Hercules, CA) with the pCSII-EF-MCS-IRES-hrGFP transfer vector [51], the pCMV-Δ8/9 packaging vector, and pcDNA-VSVG envelope coding vector (generous gift from Dr H Miyoshi, RIKEN, Tsukuba, Japan). Two days after transfection, the supernatant was harvested, passed through a 0.45-μm-pore-size filter, and then subjected to centrifugation at 4°C and 75,000 × *g* for 2 h to concentrate the virus. The virus-containing pellet was dissolved in DMEM.

To produce an MLV-based vector encoding a GFP reporter, the transfer vector pDON-AI-2-IRES-hrGFP was created by excising IRES-hrGFP from pCSII-EF- MCS-IRES-hrGFP via BamHI/HpaI digestion and inserting the DNA into the corresponding site of pDON-AI-2 (Takara Bio, Ohtsu, Japan). GP293 cells, containing a plasmid expressing MLV *gag* and *pol* genes, were transfected with pDON-AI-2-IRES-hrGFP and pcDNA-VSVG. 2 days after transfection, supernatant was harvested, and virus was concentrated.

The titer of these vectors was determined using 293T cells, and scoring of transduction was performed by flow cytometry.

An HIV-based vector encoding a neomycin resistance gene was produced by transfecting the pCMV-Δ8/9 packaging vector, pcDNA-VSVG envelope coding vector, and CSII-CMV-IRES Neo^r, which was constructed by inserting IRES and a neomycin resistance gene into CSII-CMV-MCS (a generous gift from Dr H Miyoshi, RIKEN, Tsukuba, Japan).

Single round transduction assay

The mutant cell lines and the complemented cell lines were transduced with various dilutions of the HIV GFP vector or the MLV GFP vector in the presence of 8 μg/ml of polybrene (Sigma, St Louis, MO) for 12 h before changing the medium. The infected cells were harvested two days post-infection and analyzed by flow cytometry to determine the percentage of GFP-expressing cells in each sample.

Cloning of retroviral integration sites

For cloning of retroviral integration sites by the Alu-PCR-based method, cells transduced with the HIV-based vector for 2 days were collected and the genomic DNA was obtained by standard phenol-chloroform methods with proteinase K treatment. 3' junctional sequences of HIV were amplified by 1st long PCR using a primer (HIV3-1) specific to the U5 region in the HIV LTR and a primer (Alu-1) specific to the Alu repeat sequence. The amplification products were blunted using T4 DNA Polymerase (TOYOBO, Osaka, Japan), phosphorylated using T4 Polynucleotide Kinase (TOYOBO), and circularized and/or concatemerized using T4 DNA Ligase (TOYOBO). The ligation products were amplified by 2nd long PCR using a primer (HIV3-2) specific to the U5 region in the HIV LTR and a primer (HIV3-3) spanning the junctions generated by ligation. Similarly, 5' junctional sequences of HIV were amplified by 1st PCR using a primer (HIV5-1) specific to the U3 region in the HIV LTR and a primer (Alu-2) specific to the Alu repeat sequence, and 2nd PCR using a primer (HIV5-2) specific to the U3 region in the HIV LTR and a primer (HIV5-3) spanning the junctions generated by ligation. 3' junctional sequences of MLV were amplified by 1st PCR using a primer (MLV3-1) specific to the U5 region in the MLV LTR and a primer (Alu-1) specific to Alu repeat sequence, and 2nd PCR using a primer (MLV3-2) specific to the U5 region in the MLV LTR and a primer (MLV3-3) spanning the junctions generated by ligation. The 2nd PCR products were cloned into the pGEM-T Easy Vector (Invitrogen, Carlsbad, CA), which allows for isolation of individual clones.

For cloning of integration sites including 5' and 3' ends of the same provirus, Mre11-deficient cells were transduced by the HIV-based vector encoding a neomycin resistance gene and cultured in DMEM containing 500 μg/ml G418 for a month. After DNA extraction, the genomic DNA was digested with EcoRI, circularized using T4 DNA Ligase, and digested with NotI. Then, both of the junctional sequences of HIV provirus were amplified by 1st long PCR using a primer (HIV-U5) specific to the U5 region in the HIV LTR and a primer (HIV5-1) that was previously described and 2nd long PCR using another primer (HIV3-1) that was previously described and a primer (HIV-U3) specific to the U3 region in the HIV LTR. The 2nd PCR products were cloned into the pGEM-T Easy Vector.

The sequences of the primers used in these assays are described in Additional file 3.

Sequence analysis of retroviral integration sites

Sequencing was performed using the Big Dye Terminator (version 3.1) cycle sequencing kit and an ABI3130 autosequencer (both from Applied Biosystems, Foster City, CA). The BLAT program http://genome.ucsc.edu, hosted at the University of California, Santa Cruz, was used to search each integration clone against the March 2006 freeze of the human genome. Low-quality sequences and sequences with < 20 base pairs (bp) were discarded.

Quantification of HIV-1 cDNA

HIV-1 cDNA was quantified by fluorescent-monitored quantitative PCR (Taqman) with an ABI Prism 7700 sequence detection system (Applied Biosystems) essentially as described [24]. Cells were infected with the HIV-based vector and the total DNA was extracted with DNAzol (Invitrogen) after 12 h or 24 h for analysis of total cDNA or 2-LTR and 1-LTR circles, respectively. Sequences of primers and probes are as follows; total cDNA forward, late RT F: 5'-TGTGTGCCCGTCTGTTGTGT-3'; total cDNA reverse, late RT R: 5'-GAGTCCTGCGTCGAGAGAGC-3'; total cDNA probe, LRT-P: 5'-(FAM)-CAGTGGCGCCCGAACAGGGA-(TAMRA)-3'; 2-LTR circle forward, 2-LTR F: 5'-AACTAGGGAACCCACTGCTTAAG-3'; 2-LTR reverse, 2-LTR-R: 5'-TCCACAGATCAAGGATATCTTGTC-3'; 2-LTR probe, MH603: 5'-(FAM)-ACACTACTTGAAGCACTCAAGGCAAGCTTT-(TAMRA)-3'; 1-LTR circle forward, 1-LTR F: 5'-CACACCTCAGGTACCTTTAAGA-3'; 1-LTR reverse, 1-LTR-R: 5'-GCGCTTCAGCAAGCCGAGTCCT-3'; 1-LTR probe, MH603: 5'-(FAM)-ACACTACTTGAAGCACTCAAGGCAAGCTTT-(TAMRA)-3'. Under our PCR conditions with 1-LTR-F and 1-LTR-R primers, 1-LTR circle products (~660 bp) were preferentially amplified compared with 2-LTR circle products (~1170 bp), as described previously [52]. This was verified by checking the specific amplicon generated by standard PCR with the same conditions. For standard curves, we constructed control plasmids by PCR amplification from the total DNA extracts using the same primers as fluorescent-monitored quantitative PCR and cloning the products into the pGEM-T Easy Vector.

Competing interests

The authors declare that they have no competing interests.

Authors' contributions

YS and MM designed and performed research; KK and KA contributed new reagents/analytic tools; YS, KK, and MM analyzed data; YS and MM wrote the paper.

Additional material

Additional file 1

Figure S1. Transduction efficiency of an MLV-based vector into cells deficient in DSB repair enzymes. Description: The transduction efficiency of the MLV-based vector was drastically decreased in DNA-PKcs-deficient cells and decreased in Mre11-deficient cells, but not altered in ATM- and NBS1-deficient cells. (A) ATM-deficient cells and ATM-complemented cells were transduced with the MLV-based vector encoding a GFP reporter. 2 days postinfection, the percentage of GFP-positive cells was determined by flow cytometry. (B-D) The influence of DNA-PKcs (B), NBS1 (C) and Mre11 (D) on transduction efficiency of the MLV-based vector was investigated by the same method as in (A). Error bars represent +/- SD.
Click here for file
[http://www.biomedcentral.com/content/supplementary/1742-4690-6-114-S1.PDF]

Additional file 2

Figure S2. Abnormal 3' junctions of the HIV-1 provirus in DNA-PKcs-deficient cells. Description: (A) Junctions between the 3' end of the provirus and the host DNA were analyzed in DNA-PKcs-deficient cells transduced with an HIV-based vector. Inserted abnormal sequences are in lower case. Abnormal nucleotides corresponding to the GT dinucleotides processed by integrase are presented in bold. (B) The number of junctions with insertions and/or deletions. The P values under the table are for comparison of the number of junctions with only insertions or both insertions and deletions to that of MRC5SV cells in Table 1.
Click here for file
[http://www.biomedcentral.com/content/supplementary/1742-4690-6-114-S2.PDF]

Additional file 3

Table S1. Primers for the sequence analyses around retroviral integration sites.
Click here for file
[http://www.biomedcentral.com/content/supplementary/1742-4690-6-114-S3.PPT]

Acknowledgements

We thank Dr. P. Concannon (University of Virginia, VA, USA) for providing Mre11-deficient cells, Dr H. Miyoshi (RIKEN, Tsukuba, Japan) for providing plasmids required for production of viral vectors, M. Shimada (Kyoto University, Kyoto, Japan) and M. Shirakawa (Kyoto University, Kyoto, Japan) for valuable advice, and the members of Matsuoka laboratory for helpful discussions.

This work was supported by Research Fellowships of the Japan Society for the Promotion of Science for Young Scientists.

References

1. Delelis O, Carayon K, Saib A, Deprez E, Mouscadet JF: **Integrase and integration: biochemical activities of HIV-1 integrase.** *Retrovirology* 2008, **5**:114.
2. Skalka AM, Katz RA: **Retroviral DNA integration and the DNA damage response.** *Cell Death Differ* 2005, **12(Suppl 1)**:971-978.
3. Smith JA, Daniel R: **Following the path of the virus: the exploitation of host DNA repair mechanisms by retroviruses.** *ACS Chem Biol* 2006, **1**:217-226.
4. Lavin MF, Kozlov S: **ATM activation and DNA damage response.** *Cell Cycle* 2007, **6**:931-942.
5. Kurz EU, Lees-Miller SP: **DNA damage-induced activation of ATM and ATM-dependent signaling pathways.** *DNA Repair (Amst)* 2004, **3**:889-900.
6. Zhao S, Weng YC, Yuan SS, Lin YT, Hsu HC, Lin SC, Gerbino E, Song MH, Zdzienicka MZ, Gatti RA, Shay JW, Ziv Y, Shiloh Y, Lee EY: **Functional link between ataxia-telangiectasia and Nijmegen breakage syndrome gene products.** *Nature* 2000, **405**:473-477.
7. Uziel T, Lerenthal Y, Moyal L, Andegeko Y, Mittelman L, Shiloh Y: **Requirement of the MRN complex for ATM activation by DNA damage.** *EMBO J* 2003, **22**:5612-5621.
8. Lee JH, Paull TT: **ATM activation by DNA double-strand breaks through the Mre11-Rad50-Nbs1 complex.** *Science* 2005, **308**:551-554.
9. Dupre A, Boyer-Chatenet L, Gautier J: **Two-step activation of ATM by DNA and the Mre11-Rad50-Nbs1 complex.** *Nat Struct Mol Biol* 2006, **13**:451-457.
10. O'Driscoll M, Jeggo PA: **The role of double-strand break repair - insights from human genetics.** *Nat Rev Genet* 2006, **7**:45-54.
11. Lees-Miller SP, Meek K: **Repair of DNA double strand breaks by non-homologous end joining.** *Biochimie* 2003, **85**:1161-1173.
12. Sekiguchi JM, Ferguson DO: **DNA double-strand break repair: a relentless hunt uncovers new prey.** *Cell* 2006, **124**:260-262.
13. Ma Y, Pannicke U, Schwarz K, Lieber MR: **Hairpin opening and overhang processing by an Artemis/DNA-dependent protein kinase complex in nonhomologous end joining and V(D)J recombination.** *Cell* 2002, **108**:781-794.
14. Daniel R, Katz RA, Skalka AM: **A role for DNA-PK in retroviral DNA integration.** *Science* 1999, **284**:644-647.
15. Jeanson L, Subra F, Vaganay S, Hervy M, Marangoni E, Bourhis J, Mouscadet JF: **Effect of Ku80 depletion on the preintegrative steps of HIV-1 replication in human cells.** *Virology* 2002, **300**:100-108.
16. Daniel R, Greger JG, Katz RA, Taganov KD, Wu X, Kappes JC, Skalka AM: **Evidence that stable retroviral transduction and cell survival following DNA integration depend on components of the nonhomologous end joining repair pathway.** *J Virol* 2004, **78**:8573-8581.
17. Lau A, Swinbank KM, Ahmed PS, Taylor DL, Jackson SP, Smith GC, O'Connor MJ: **Suppression of HIV-1 infection by a small molecule inhibitor of the ATM kinase.** *Nat Cell Biol* 2005, **7**:493-500.
18. Brin E, Yi J, Skalka AM, Leis J: **Modeling the late steps in HIV-1 retroviral integrase-catalyzed DNA integration.** *J Biol Chem* 2000, **275**:39287-39295.
19. Yoder KE, Bushman FD: **Repair of gaps in retroviral DNA integration intermediates.** *J Virol* 2000, **74**:11191-11200.
20. Li L, Olvera JM, Yoder KE, Mitchell RS, Butler SL, Lieber M, Martin SL, Bushman FD: **Role of the non-homologous DNA end joining pathway in the early steps of retroviral infection.** *EMBO J* 2001, **20**:3272-3281.
21. Kilzer JM, Stracker T, Beitzel B, Meek K, Weitzman M, Bushman FD: **Roles of host cell factors in circularization of retroviral dna.** *Virology* 2003, **314**:460-467.
22. Smith JA, Wang FX, Zhang H, Wu KJ, Williams KJ, Daniel R: **Evidence that the Nijmegen breakage syndrome protein, an early sensor of double-strand DNA breaks (DSB), is involved in HIV-1 post-integration repair by recruiting the ataxia telangiectasia-mutated kinase in a process similar to, but distinct from, cellular DSB repair.** *Virol J* 2008, **5**:11.
23. Taganov K, Daniel R, Katz RA, Favorova O, Skalka AM: **Characterization of retrovirus-host DNA junctions in cells deficient in nonhomologous-end joining.** *J Virol* 2001, **75**:9549-9552.
24. Butler SL, Hansen MS, Bushman FD: **A quantitative assay for HIV DNA integration in vivo.** *Nat Med* 2001, **7**:631-634.
25. Ma Y, Pannicke U, Lu H, Niewolik D, Schwarz K, Lieber MR: **The DNA-dependent protein kinase catalytic subunit phosphorylation sites in human Artemis.** *J Biol Chem* 2005, **280**:33839-33846.
26. Chen L, Morio T, Minegishi Y, Nakada S, Nagasawa M, Komatsu K, Chessa L, Villa A, Lecis D, Delia D, Mizutani S: **Ataxia-telangiectasia-mutated dependent phosphorylation of Artemis in response to DNA damage.** *Cancer Sci* 2005, **96**:134-141.
27. Carteau S, Hoffmann C, Bushman F: **Chromosome structure and human immunodeficiency virus type 1 cDNA integration: centromeric alphoid repeats are a disfavored target.** *J Virol* 1998, **72**:4005-4014.
28. Holman AG, Coffin JM: **Symmetrical base preferences surrounding HIV-1, avian sarcoma/leukosis virus, and murine**

leukemia virus integration sites. *Proc Natl Acad Sci USA* 2005, **102**:6103-6107.
29. Derse D, Crise B, Li Y, Princler G, Lum N, Stewart C, McGrath CF, Hughes SH, Munroe DJ, Wu X: **Human T-cell leukemia virus type 1 integration target sites in the human genome: comparison with those of other retroviruses.** *J Virol* 2007, **81**:6731-6741.
30. Sherman PA, Fyfe JA: **Human immunodeficiency virus integration protein expressed in Escherichia coli possesses selective DNA cleaving activity.** *Proc Natl Acad Sci USA* 1990, **87**:5119-5123.
31. Pullen KA, Ishimoto LK, Champoux JJ: **Incomplete removal of the RNA primer for minus-strand DNA synthesis by human immunodeficiency virus type 1 reverse transcriptase.** *J Virol* 1992, **66**:367-373.
32. Smith JS, Roth MJ: **Specificity of human immunodeficiency virus-1 reverse transcriptase-associated ribonuclease H in removal of the minus-strand primer, tRNA(Lys3).** *J Biol Chem* 1992, **267**:15071-15079.
33. Maser RS, DePinho RA: **Telomeres and the DNA damage response: why the fox is guarding the henhouse.** *DNA Repair (Amst)* 2004, **3**:979-988.
34. Cenci G, Ciapponi L, Gatti M: **The mechanism of telomere protection: a comparison between Drosophila and humans.** *Chromosoma* 2005, **114**:135-145.
35. Rooney S, Alt FW, Lombard D, Whitlow S, Eckersdorff M, Fleming J, Fugmann S, Ferguson DO, Schatz DG, Sekiguchi J: **Defective DNA repair and increased genomic instability in Artemis-deficient murine cells.** *J Exp Med* 2003, **197**:553-565.
36. Stracker TH, Theunissen JW, Morales M, Petrini JH: **The Mre11 complex and the metabolism of chromosome breaks: the importance of communicating and holding things together.** *DNA Repair (Amst)* 2004, **3**:845-854.
37. Konig R, Zhou Y, Elleder D, Diamond TL, Bonamy GM, Irelan JT, Chiang CY, Tu BP, De Jesus PD, Lilley CE, Seidel S, Opaluch AM, Caldwell JS, Weitzman MD, Kuhen KL, Bandyopadhyay S, Ideker T, Orth AP, Miraglia LJ, Bushman FD, Young JA, Chanda SK: **Global analysis of host-pathogen interactions that regulate early-stage HIV-1 replication.** *Cell* 2008, **135**:49-60.
38. Baekelandt V, Claeys A, Cherepanov P, De Clercq E, De Strooper B, Nuttin B, Debyser Z: **DNA-Dependent protein kinase is not required for efficient lentivirus integration.** *J Virol* 2000, **74**:11278-11285.
39. Daniel R, Katz RA, Merkel G, Hittle JC, Yen TJ, Skalka AM: **Wortmannin potentiates integrase-mediated killing of lymphocytes and reduces the efficiency of stable transduction by retroviruses.** *Mol Cell Biol* 2001, **21**:1164-1172.
40. Daniel R, Kao G, Taganov K, Greger JG, Favorova O, Merkel G, Yen TJ, Katz RA, Skalka AM: **Evidence that the retroviral DNA integration process triggers an ATR-dependent DNA damage response.** *Proc Natl Acad Sci USA* 2003, **100**:4778-4783.
41. Dehart JL, Andersen JL, Zimmerman ES, Ardon O, An DS, Blackett J, Kim B, Planelles V: **The ataxia telangiectasia-mutated and Rad3-related protein is dispensable for retroviral integration.** *J Virol* 2005, **79**:1389-1396.
42. Ariumi Y, Turelli P, Masutani M, Trono D: **DNA damage sensors ATM, ATR, DNA-PKcs, and PARP-1 are dispensable for human immunodeficiency virus type 1 integration.** *J Virol* 2005, **79**:2973-2978.
43. Llano M, Saenz DT, Meehan A, Wongthida P, Peretz M, Walker WH, Teo W, Poeschla EM: **An essential role for LEDGF/p75 in HIV integration.** *Science* 2006, **314**:461-464.
44. Zielske SP, Stevenson M: **Modest but reproducible inhibition of human immunodeficiency virus type 1 infection in macrophages following LEDGFp75 silencing.** *J Virol* 2006, **80**:7275-7280.
45. Llano M, Vanegas M, Fregoso O, Saenz D, Chung S, Peretz M, Poeschla EM: **LEDGF/p75 determines cellular trafficking of diverse lentiviral but not murine oncoretroviral integrase proteins and is a component of functional lentiviral preintegration complexes.** *J Virol* 2004, **78**:9524-9537.
46. Ciuffi A, Llano M, Poeschla E, Hoffmann C, Leipzig J, Shinn P, Ecker JR, Bushman F: **A role for LEDGF/p75 in targeting HIV DNA integration.** *Nat Med* 2005, **11**:1287-1289.
47. Vandegraaff N, Devroe E, Turlure F, Silver PA, Engelman A: **Biochemical and genetic analyses of integrase-interacting proteins lens epithelium-derived growth factor (LEDGF)/p75 and hepatoma-derived growth factor related protein 2 (HRP2) in preintegration complex function and HIV-1 replication.** *Virology* 2006, **346**:415-426.
48. Kobayashi N, Agematsu K, Sugita K, Sako M, Nonoyama S, Yachie A, Kumaki S, Tsuchiya S, Ochs HD, Sugita K, Fukushima Y, Komiyama A: **Novel Artemis gene mutations of radiosensitive severe combined immunodeficiency in Japanese families.** *Hum Genet* 2003, **112**:348-352.
49. Sakamoto S, Iijima K, Mochizuki D, Nakamura K, Teshigawara K, Kobayashi J, Matsuura S, Tauchi H, Komatsu K: **Homologous recombination repair is regulated by domains at the N- and C-terminus of NBS1 and is dissociated with ATM functions.** *Oncogene* 2007, **26**:6002-6009.
50. Takai K, Sakamoto S, Sakai T, Yasunaga J, Komatsu K, Matsuoka M: **A Potential Link between Alternative Splicing of the NBS1 Gene and DNA Damage/Environmental Stress.** *Radiat Res* 2008, **170**:33-40.
51. Kuwata H, Watanabe Y, Miyoshi H, Yamamoto M, Kaisho T, Takeda K, Akira S: **IL-10-inducible Bcl-3 negatively regulates LPS-induced TNF-alpha production in macrophages.** *Blood* 2003, **102**:4123-4129.
52. Jacque JM, Stevenson M: **The inner-nuclear-envelope protein emerin regulates HIV-1 infectivity.** *Nature* 2006, **441**:641-645.

Femoral Osteomyelitis due to *Cladophialophora arxii* in a Patient with Chronic Granulomatous Disease

T. Shigemura, K. Agematsu, T. Yamazaki, K. Eriko, G. Yasuda, K. Nishimura, K. Koike

Abstract
Fungal infections in patients with chronic granulomatous disease (CGD) are a poor prognostic factor. We describe the first case of CGD with femoral osteomyelitis due to *Cladophialophora arxii*, which is a member of the dematiaceous group. The causative fungus was identified on the basis of its morphological characteristics, growth temperature profile, and nucleotide sequence on the internal transcribed space region of the ribosomal gene. The patient was successfully treated with surgical debridement, subsequent administration of itraconazolem and interferon-γ.

Infection 2009; 37: 469–473
DOI 10.1007/s15010-009-8238-9

Introduction

Chronic granulomatous disease (CGD) is a rare, inherited primary immunodeficiency disease that results from defects in phagocytic cells associated with the low activity of nicotinamide adenine dinucleotide phosphate (NADPH) oxidase [1]. CGD patients are susceptible to infections, especially those caused by catalase-producing bacteria, such as *Staphylococcus*, *Burkholderia*, *Serratia*, and *Nocardia*, and fungi, such as *Aspergillus* species [2]. Dematiaceous fungi, such as *Cladophialophora arxii*, which are characterized by black melanin pigment, are isolated less frequently in CGD patients.

We report a patient with CGD who developed femoral osteomyelitis due to *C. arxii*. The patient underwent a successful treatment with surgical debridement and administration of itraconazole and IFN-γ.

Case Report

The patient was 20-year-old man with X-linked CGD. The diagnosis of CGD had been established at the age of 6 years, at which time he presented with cervical lymphadenitis, BCG lymphadenitis, a perirectal abscess, and recurrent pneumonia; the neutrophil nitroblue tetrazolium reduction was abnormal. He was treated with prophylactic therapy consisting of trimethoprim–sulfamethoxazole and oral itraconazole capsules (100 mg once daily) and developed no other serious infections until 20 years of age. However, pulmonary granulomas had been formed following an episode of pneumonia at the age of 7 years, and these had remained, gradually growing during the following 13 years. He occasionally had hemoptysis.

The patient presented with an approximately 2-week history of pain in the posterior, distal left thigh without fever. On admission, he complained of knee pain that made walking difficult. Laboratory findings included a leukocyte count of 3,950/μl, with 76% neutrophils; C-reactive protein (CRP) level, 13.8 mg/l; erythrocyte sedimentation rate, 23 mm/h; ß-D-glucan (ß-glucan Wako), 14.78 pg/ml (normal range < 11 pg/ml). Before this episode, ß-D-glucan levels had been negative. Aspergillus DNA and *Aspergillus galactomannan* antigen in the blood were undetectable. Blood cultures showed no growth.

A roentgenogram of the painful area showed no abnormalities, but magnetic resonance imaging suggested osteomyelitis (Figure 1). A computerized tomography scan of the chest revealed a 2.5-cm nodule in the right hilar region, which partly compressed the bronchial tube, a 1.5-cm nodule in the left upper lobe, and numerous small nodules scattered throughout both lungs. Enlarged lymph nodes with calcification in the superior mediastinum, left axilla, and hepatic portal region were present. Empiric therapy with an oral itraconazole solution (200 mg once daily) and iv injection of micafungin (250 mg per day) was started because the clinical and laboratory findings suggested fungal osteomyelitis. The plasma itraconazole concentration measured with by high performance liquid chromatography, which was 626.0 ng/ml on admission, had elevated to 2,573.4 ng/ml by the third day of hospitalization. The following day, extensive surgical debridement of the lesion was performed. Pus discharge from the bone marrow was observed following the drilling of a hole in the cortex. Fungal elements were seen in the necrotic bone tissue. The culture of this specimen on Sabouraud

T. Shigemura *(corresponding author)*, **K. Agematsu, T. Yamazaki, K. Koike**
Dept. of Pediatrics, Shinshu University School of Medicine, 3-1-1 Asahi, Matsumoto, Nagano, 390-8621, Japan; Phone: (+81/263) 37-2642, Fax: -3089, e-mail: tomonari@shinshu-u.ac.jp
K. Eriko
Dept. of Laboratory Medicine, Shinshu University School of Medicine, Matsumoto, Nagano, Japan
G. Yasuda
Dept. of Orthopaedic Surgery, Shinshu University School of Medicine, Matsumoto, Nagano, Japan
K. Nishimura
First Laboratories Co., Ltd., Medical Mycology Research Center, Chiba University, Chiba, Japan

Received: June 18, 2008 · Revision accepted: February 26, 2009
Published online: August 7, 2009

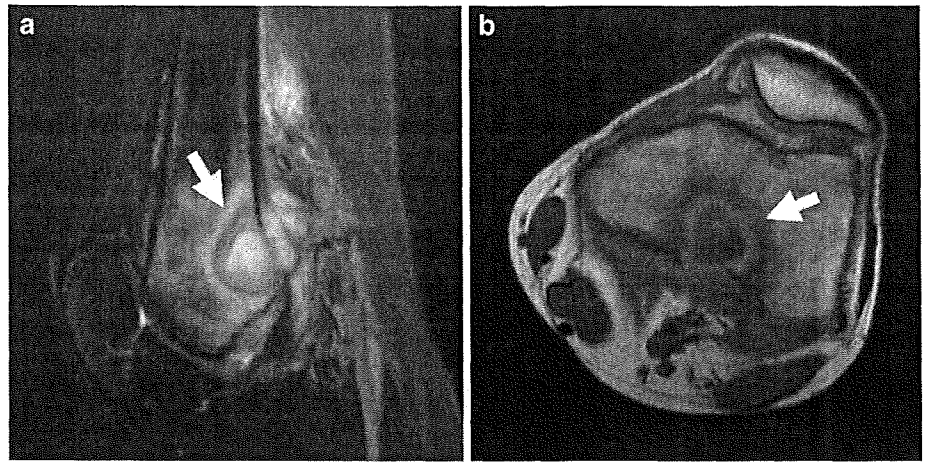

Figure 1. Magnetic resonance imaging of the distal metaphysis of the left femur before treatment. The *arrow* indicates the site of the lesion. a. Sagittal section. b. Coronal section.

dextrose agar (Becton Dickinson Microbiology Systems, Tokyo, Japan) yielded several colonies with no bacteria present after 14 days. These colonies were dark gray and consisted of septate hyphae with smooth oval conidia. At this point, the fungus was tentatively identified as *Cladosporium* species. The patient showed clinical and laboratory signs of improvement on the 14th day of hospitalization. Therapy with itraconazole and micafungin was continued, but the level of inflammatory markers rose gradually (CRP from 2.7 to 10.5 mg/l), and the plasma itraconazole concentration decreased to 1,596.6 ng/ml. IFN-γ therapy (25 $\mu g/m^2$ two times per week) was added to the therapeutic regimen on the 24th day, and the route of itraconazole administration was changed on the 25th day, with new treatment consisting of itraconazole iv for 12 days (200 mg once daily) followed by oral capsules (200 mg twice daily). These changes in the patient's therapeutic regimen increased the plasma itraconazole concentration to over 5,000 ng/ml and decreased the CRP level to within the normal range. Micafungin was discontinued on the day of discharge (40th day after admission), while treatment with itraconazole and IFN-γ was continued. The plasma itraconazole levels stayed within the range of 7,000–8,000 ng/ml. Five months after surgery, the patient had no signs of recurrent disease, but there was little change in the pulmonary granulomas. There were no side effects as a result of the drugs given.

At the time of discharge, we had identified the isolated fungus as *C. arxii*. The MICs of itraconazole, micafungin, amphotericin B, voriconazole, flucytosine, miconazole, and fluconazole against the present isolate were 0.03 mg/l, 0.125 mg/l, 0.25 mg/l, 0.5 mg/l, 1 mg/l, 1 mg/l, and 64 mg/l, respectively. The MICs were established after 5 days of incubation and determined by the ASTY (Kyokuto Pharmaceutical Industrial Co, Tokyo, Japan) colorimetric microdilution testing system [3]. Neutrophil superoxide production on flow cytometric analysis with dihydrorhodamine 123 was 0.3% of that of control neutrophils before IFN-γ therapy. Despite continuous IFN-γ therapy, periodic clinical examinations revealed no increase in superoxide production by the patient's neutrophils.

Mycological Examination

Colonies of the causative fungus grew slowly, attaining a diameter of approximately 40 mm and 36 mm on synthetic defined agar (SDA; Difco, Detroit, MI) and potato dextrose agar (PDA; Difco) plates, respectively, at 25 °C after 35 days. They were dark grayish with aerial hyphae and blackish brown with creeping hyphae at the margin on SDA (Figure 2a) and blackish brown, felty with radial furrows on PDA. The hyphae were septate and olivaceous brown and produced laterally and terminally acropetal conidial chains that branched profusely. The conidia were pale brown to brown, smooth- and somewhat thick-walled, lemon- to spindle-shaped, and 5–13 × 3–4 µm with hila (Figure 2b). The isolate had restricted growth at 35 °C, barely grew at 37 °C and did not grow at all at 40 °C.

DNA was extracted by the benzyl chloride method from isolates cultured on PDA at 25 °C for 7 days, and the internal transcribed spacer (ITS) region including 5.8 S of ribosomal RNA gene (ITS1-5.8S-ITS2 rRNA) was amplified with the primer pair ITS5 (5′-GGA AGTAAAAGTCGTAACAAGG-3′) and ITS4 (5′-TCCTCCGCTTATTGATATG-3′). The PCR products were labeled by ITS1 (5′-TCCGTAGGTGAACCTGC GG-3′) and ITS4. A total of 528 bases were determined, and these showed a 98% homology against the ITS region in *C. arxii* IFM 52022 (Accession No. AB109181), derived from the type strain CBS 306.94.

Based on these results, the causative fungus was identified as *C. arxii*, and the sequence was registered at DNA Data Bank of Japan (DDBJ), National Institute of Genetics as Accession No. AB458597.

Discussion

CGD patients have frequent life-threatening bacterial and fungal infections because superoxide production is decreased in their phagocytes [1]. Such patients usually suffer from infections of the skin, lymph nodes, lungs, liver, and gastrointestinal tract, with the lungs being the most common sites of infections. The overall incidence of fungal infections has been reported to be 20% among patients with CGD [4]. *Aspergillus* species are the most common cause of fungal infections, but there have been a few reports of other infections caused by other fungal species. Although pulmonary infections due to *Aspergillus* species are common, fungal osteomyelitis due to *Aspergillus* species is uncommon. In particular, long bone osteomyelitis due to non-*Aspergillus* fungi has been re-

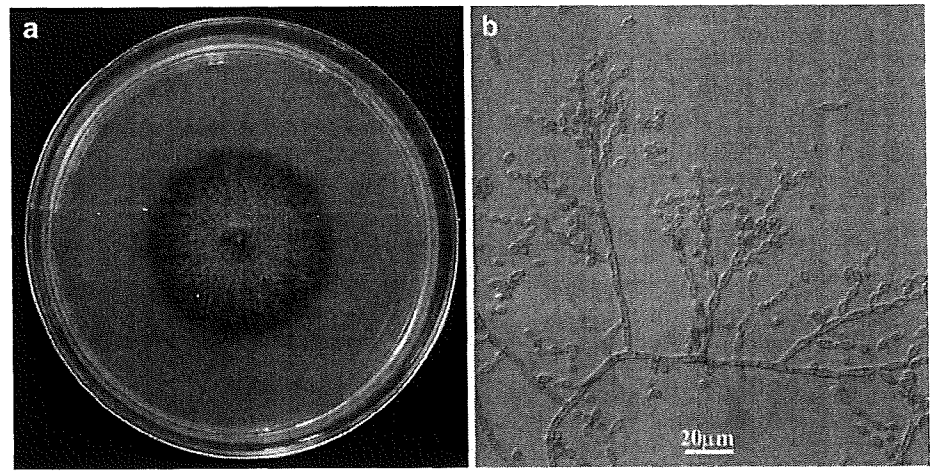

Figure 2. a. Colony on synthetic defined agar plate after a 35-day incubation at 25 °C. b. Micrograph from a slide culture on potato dextrose agar showing branching conidial chains and liberated conidia.

ported only rarely [5]. Osteomyelitis may be a part of a systemic infection, or it may be the only localized focus of infection. In the case reported here, the patient had pulmonary granulomas that partly compressed the bronchial tube as well as hemoptysis on occasion. We hypothesized that the causative fungus disseminated into the bone lesion through the bloodstream from the lung lesion, which may have been caused by air–bone infection. Therefore, we expected that itraconazole therapy would at least diminish the size of the pulmonary granulomas that had formed during the preceding 13 years. However, this therapy did not result in such a favorable response.

Cladophialophora arxii is a relatively new member of the dematiaceous group of mycelial fungal pathogens, being reported as a new species of the genus *Cladophialophora* in 1995 [6]. The identification of this species is often difficult because of its rarity and morphological similarity to some other *Cladophialophora* species. The morphology of the conidial system of *C. arxii* is very similar to that of *Cladophialophora devriesii*, and *C. devriesii* also grows at 37 °C but not at 40 °C. However, the conidial chains of the fungus isolated from our patient are slightly longer than those of *C. devriesii*, and the identity of the ITS region of the rRNA gene shows only an 89–90% similarity with *C. devriesii*. Even though the growth temperature profile is similar to that of *C. devriesii*, the conidial morphology and DNA identity strongly suggest that the present isolate is *C. arxii* and not *C. devriesii*. Generally speaking, maximum growth temperatures (MaxGT) of the dematiaceous fungi are not strict; for example, the MaxGT of a principal dematiaceous fungal pathogen, *Fonsecaea prodrosoi*, ranges from 38 °C to 42 °C. The MaxGT of *C. arxii* for most isolates is probably in the range of 37–40 °C. Thus, the fungus isolated from our patient can be clearly differentiated by conidial morphology, MaxGT, and identity (88%) on the ITS region from *C. bantiana*, which is characterized by long ellipsoidal or nearly cylindrical conidia consisting of very long, poorly branched chains and good growth at 37 °C (MaxGT 40–45 °C). The identification of such a rare and slow-growing fungus is time-consuming and requires expert knowledge of the morphology and physiology of the fungus. Consequently, an analysis of the ITS region on the rRNA gene facilitates an early diagnosis and species differentiation. However, we have to be careful when accessing the names of fungi with sequence identities using the nucleotide databases of NCBI BLAST (National Center for Biotechnology Information, Basic Local Alignment Search Tool; National Institutes of Health, Bethesda, MDA). The fungal listings in these databases sometimes mention several or more names of fungi that actually belong to different genera or species. In order to obtain the correct name for a fungus, especially a filamentous one, morphological, physiological, and biochemical studies should be carried out simultaneously.

Dematiaceous fungi have been recognized as etiologic agents of phaeohyphomycosis, chromoblastomycosis, and eumycotic mycetoma. Although disseminated infection caused by dematiaceous fungi is uncommon, it has been increasingly recognized as a cause of serious disease, especially in immunodeficient patients. Brain abscesses due to *C. bantiana* are the commonest form of systemic phaeohyphomycosis [7]. Other localized deep forms of infections, such as arthritis [8], endocarditis [9], and osteomyelitis [10], have been rarely reported. *Cladophialophora devriesii* is a very rare pathogen and reported to have caused fatal dissemination [11, 12]. Our patient had femoral osteomyelitis due to *C. arxii*. To the best of our knowledge, this is the first documented case of osteomyelitis caused by a dematiaceous fungus in CGD patients. In addition, *C. arxii* is an extremely rare species, and this is only the second reported case of *C. arxii* infection in humans.

Although guidelines for treatment of fungal osteomyelitis due to non-*Aspergillus* fungi are not well established, surgery generally plays an important role in the

management of CGD patients [13]. In cases of *Aspergillus* osteomyelitis, surgical debridement appears to be very important for a successful treatment, and extensive debridement is more effective than limited intralesional debridement [14]. Invasive fungal infections are a major cause of morbidity and mortality in CGD patients, and other rare and emerging fungi can cause significant diseases. The treatment of fungal infections involves the prolonged use of systemic antifungal agents and, in some cases, the causative fungi may be refractory to antifungal treatment. Therefore, extensive surgical debridement is also likely to be necessary in cases of non-*Aspergillus* fungi osteomyelitis.

Itraconazole has a broad spectrum of activity against many infections caused by pathogenic fungi, and it is well tolerated and safe [15]. Prophylactic itraconazole is effective in preventing fungal infection in CGD patients [16]. However, low plasma itraconazole concentrations can cause a failure of prophylaxis or treatment. The absorption of itraconazole when given as a capsule formulation is highly variable [17]; for example, adequate absorption requires an acid gastric environment and the presence of food.

In the case reported here, we selected itraconazole regardless of the patient suffering from fungal infection during itraconazole prophylaxis. This choice of treatment was based on the evidence that the CRP level, which had persisted at > 10 mg/l for more than 2 weeks before admission, decreased from 13.8 mg/l to 6.6 mg/l and the ß-d-glucan became negative (< 3.57 pg/ml) following an increase in itraconazole from 100 mg to 200 mg during the 4 days until the diagnosis was made. In fact, the MIC of itraconazole was low and itraconazole had good in vitro activity against the fungus isolated. Although the MIC of itraconazole was very low (0.03 mg/l), the patient developed fungal osteomyelitis during itraconazole prophylaxis. In general, in vitro susceptibility testing for slow-growing organisms are problematic and not standardized [18]. The MICs of the present isolate were established after 5 days of incubation, but true MIC endpoints may have needed a longer incubation time because the isolated fungus grew extremely slowly. Furthermore, antifungal pharmacodynamic parameters in RPMI-1640, which is the standard synthetic medium for in vitro antifungal susceptibility testing, may not always predict antifungal activity in serum for azoles. In particular, highly protein-bound antifungal agents, such as itraconazole (protein binding, 99.8%), have a trend toward higher MICs in the presence of serum [19]. In addition, the patient had taken prophylactic itraconazole capsules without food for several months before hospitalization. As a result, plasma concentrations of itraconazole may have decreased. Thus, we attribute the failure of the prophylaxis to decreasing plasma concentrations of itraconazole. Therapy with escalating concentrations of itraconazole resulted in improved laboratory test results. Plasma itraconazole concentrations should be measured when there is failure of prophylaxis or treatment.

This is the first reported case of osteomyelitis due to dematiaceous fungi in CGD patients. The causative agent was found to be an extremely rare microorganism, *C. arxii*. The patient was successfully treated with surgical debridement, increasing concentrations of itraconazole, and IFN-γ treatment.

Acknowledgments

The authors would like to thank Dr. Ayako Sano, Medical Mycology Research Center, Chiba University, Japan for her assistance in registering the nucleotide sequence to DDBJ.

References

1. Segal BH, Leto TL, Gallin JI, Malech HL, Holland SM: Genetic, biochemical, and clinical features of chronic granulomatous disease. Medicine (Baltimore) 2000; 79: 170–200.
2. Winkelstein JA, Marino MC, Johnston RB Jr, Boyle J, Curnutte J, Gallin JI, Malech HL, Holland SM, Ochs H, Quie P, Buckley RH, Foster CB, Chanock SJ, Dickler H: Chronic granulomatous disease. Report on a national registry of 368 patients. Medicine (Baltimore) 2000; 79: 155–169.
3. Pfaller MA, Arikan S, Lozano-Chiu M, Chen Y, Coffman S, Messer SA, Rennie R, Sand C, Heffner T, Rex JH, Wang J, Yamane N: Clinical evaluation of the ASTY colorimetric microdilution panel for antifungal susceptibility testing. J Clin Microbiol 1998; 36: 2609–2612.
4. Cohen MS, Isturiz RE, Malech HL, Root RK, Wilfert CM, Gutman L, Buckley RH: Fungal infection in chronic granulomatous disease. The importance of the phagocyte in defense against fungi. Am J Med 1981; 71: 59–66.
5. Sponseller PD, Malech HL, McCarthy EF Jr, Horowitz SF, Jaffe G, Gallin JI: Skeletal involvement in children who have chronic granulomatous disease. J Bone Joint Surg Am 1991; 73: 37–51.
6. Tintelnot K, von Hunnius P, de Hoog GS, Polak-Wyss A, Gueho E, Masclaux F: Systemic mycosis caused by a new *Cladophialophora* species. J Med Vet Mycol 1995; 33: 349–354.
7. Revankar SG, Sutton DA, Rinaldi MG: Primary central nervous system phaeohyphomycosis: a review of 101 cases. Clin Infect Dis 2004; 38: 206–216.
8. Ziza JM, Dupont B, Boissonnas A, Meyniard O, Bedrossian J, Drouhet E, Cremer GA: [Osteoarthritis caused by dematiaceous fungi. Apropos of 3 cases]. Ann Med Interne (Paris) 1985; 136: 393–397.
9. Gavin PJ, Sutton DA, Katz BZ: Fatal endocarditis in a neonate caused by the dematiaceous fungus *Phialemonium obovatum*: case report and review of the literature. J Clin Microbiol 2002; 40: 2207–2212.
10. Sharma NL, Mahajan V, Sharma RC, Sharma A: Subcutaneous pheohyphomycosis in India – a case report and review. Int J Dermatol 2002; 41: 16–20.
11. Gonzalez MS, Alfonso B, Seckinger D, Padhye AA, Ajello L: Subcutaneous phaeohyphomycosis caused by *Cladosporium devriesii*, sp. nov. Sabouraudia 1984; 22: 427–432.
12. Mitchell DM, Fitz-Henley M, Horner-Bryce J: A case of disseminated phaeohyphomycosis caused by *Cladosporium devriesii*. West Indian Med J 1990; 39: 118–123.